Electronic Supplementary Information

Phototactic Micromotor Assemblies in Dynamic Line Formations for Wide-Range Micromanipulations

Xia Guo[‡], Yukuan Wang[‡], Fangzhi Mou, Qi Xie, Shu Su, Chuanrui Chen, and Jianguo Guan**

State Key Laboratory of Advanced Technology for Materials Synthesis and Processing, International School of Materials Science and Engineering, Wuhan University of Technology, 122 Luoshi Road, Wuhan 430070 (P.R. China)

KEYWORDS. Micro/nanomotors, collective behaviors, formation control, magnetic assembly, phototaxis, micromanipulation

Experimental Section

Materials

Anhydrous ethanol (CH_3CH_2OH), tetrabutyl titanate ($C_{16}H_{36}O_4Ti$), hydrogen peroxide solution (H_2O_2), ethylene glycol($C_2H_6O_2$) were purchased from Sinopharm Chemical Reagent Co., Ltd. (China). All chemicals were all of the analytic grades and were used without further purification. Hydroxyl Magnetic Beads (500 nm) were purchased from Suzhou Nano-Micro Technology Co., Ltd. (Suzhou, China). Polystyrene (PS) microspheres (5 μm) were purchased from Aladdin-Holdings Group.

Fabrication of MB@TiO_2 MMs

The MB@TiO_2 MMs were synthesized by an ultrasonic-assisted sol-gel method. At first, a 176 μL tetrabutyl titanate and 5 mL ethylene glycol were mixed and magnetically stirred for 10 min. Then, a 5 mL ethanol suspension of magnetic beads (MBs, 2 mg mL^{-1}) was added to the above solution and sonicated for 20 min in an ultrasonic cleaner (Sumei KQ2200, China). After being collected by magnetic separation and washed three times with deionized water and absolute ethanol, MB@amorphous TiO_2 core-shell microparticles (MB@A-TiO_2 MPs) were obtained. Finally, the MB@A-TiO_2 MPs were calcined at 550 °C for 2 h to obtain the MB@TiO_2 MMs.

Characterization

Scanning electron microscopy (SEM) images were obtained using a Hitachi S-4800 field-emission SEM (Japan). Transmission electron microscopy (TEM) images were obtained using a High-resolution Transmission Electron Microscope (JEM-1400Plus, Japan). The zeta potential of the MMs was obtained by NanoBrook 90 Plus Zeta (US). An X-ray photoelectron spectroscopy (XPS) (Thermo Scientific ESCALAB 250Xi, USA) was employed to characterize the XPS spectra of Ti 2p on the MB@TiO_2 MMs. The magnetization hysteresis loop of the MB@TiO_2 MMs was acquired by a vibrating sample magnetometer (LakeShore 7404, USA) at room temperature. A digital Tesla meter (YF-801EXP, China) was used to measure the intensity of the applied magnetic field.

Phototactic flocking behaviors and cooperative large-cargo manipulations

A 65 μL of the aqueous suspension of MB@TiO_2 MMs (0.4 mg mL^{-1}) and a 65 μL of H_2O_2 solution (5 wt.%) were dropped onto a clean glass slide and covered with a cover glass. UV lamps with a wavelength of 365 nm and intensity (I) of 0.41 W cm^{-2} (SZ Lamplic Technology) were used as the sidewise light sources, which were set above the substrate and irradiated downward with an oblique incident angle of 30°. The UV light from the built-in Leica EL6000 light source of an inverted optical microscope (Leica DMI 3000B, Germany) was used as the vertical light source (UV_z, I = 0.51 W cm^{-2}) to avoid floating up of the MMs. A permanent magnet was placed next to the slide to provide a static magnetic field (H). The assembly/disassembly and phototactic flocking behaviors of the MB@TiO_2 MMs were investigated by controlling the on/off states, directions and intensity of the sidewise light sources and the applied H. The PS microspheres with a size of 5 μm were used as large cargoes to investigate their cooperative large-cargo manipulations. Micropatterned glass chips with rectangular prism obstacles, Y-shaped branched microchannels or dumbbell-shape microchannels were used to investigate the phototactic flocking behaviors and cooperative large-cargo manipulations of the MB@TiO_2 MMAs in complex microenvironments. All videos were recorded at room temperature by an inverted optical microscope (Leica DMI 3000B, Germany) and analyzed by using ImageJ and Video Spot Tracker V08.01 software.

Numerical simulation

The simulations were performed by using the diffusions, electrostatics and creeping flow modules of COMSOL Multiphysics software.[1] In the simulation, a two-dimensional (2D) model was built up by placing an MB@TiO_2 MMA in the middle of a cuboid cell (20×20 μm) filled with water. The release and consumption rate of H^+ on the illuminated and shadowed surface of the MB@TiO_2 MMA was set to be 1×10^{-8} mol m^{-2} s^{-1}, respectively. The diffusion coefficient (D) of H^+ and OH^- was set to be 9.31×10^{-9} and 5.27×10^{-9} m^2 s^{-1}. The electroosmotic-flow boundary conditions were set at the charged surfaces of the MB@TiO_2 MMA and the glass substrate (the bottom edge of the cell). The zeta potential ζ_p of the MB@TiO_2 MMA was set to be -53.8 mV according to the result of the zeta potential test, and that of the glass substrate (ζ_w) was set to be -85 mV.[2]

Supplementary Figures

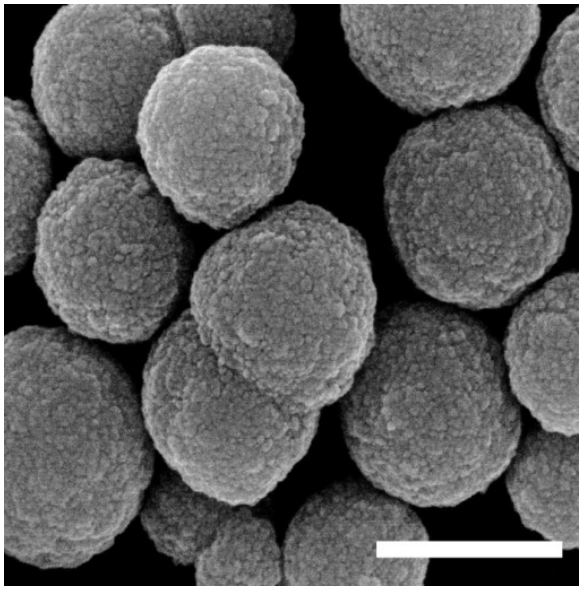

Fig. S1 The SEM image of pristine MBs. Scale bar, 500 nm.

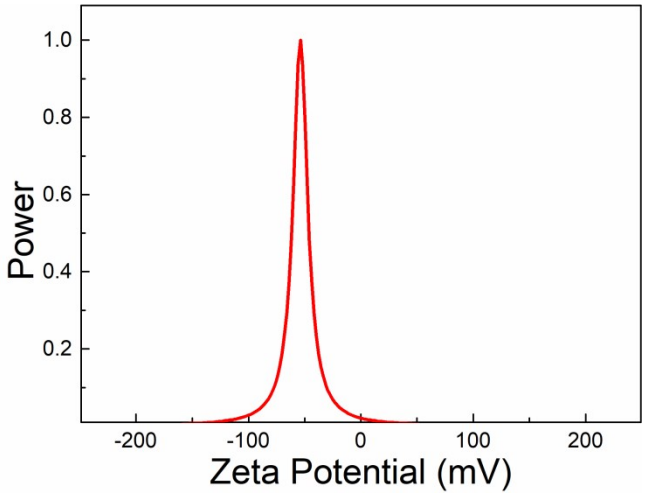

Fig. S2 The zeta potential of the MB@TiO_2 MMs.

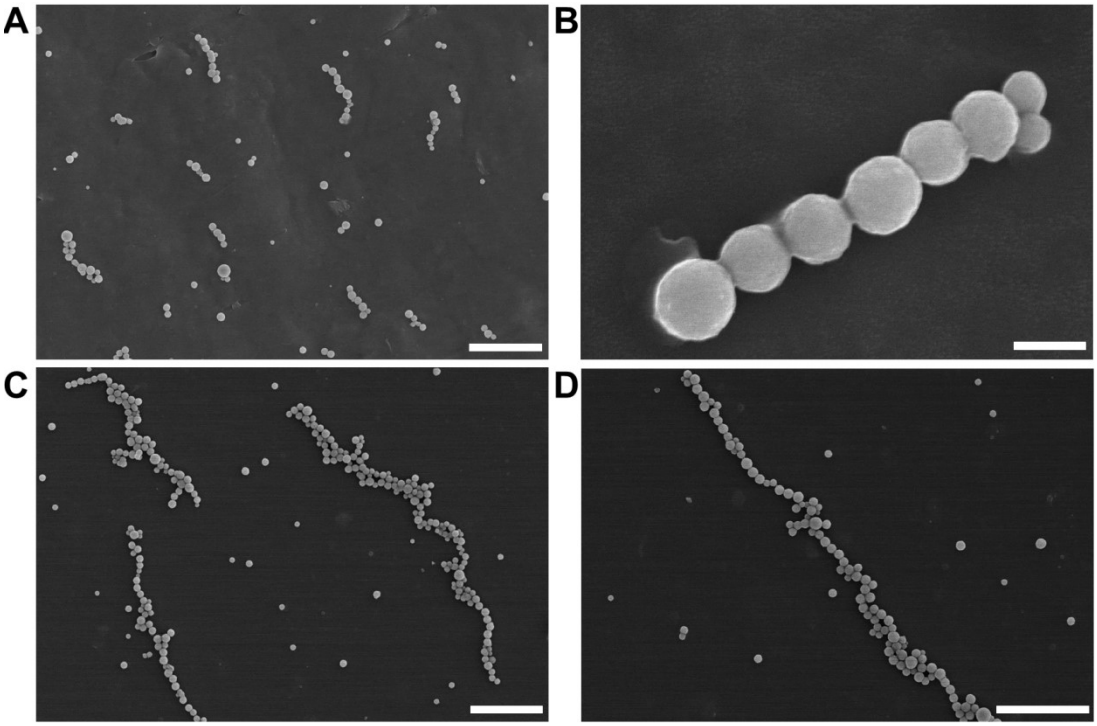

Fig. S3 SEM images of the MB@TiO_2 MMAs formed under the magnetic field with an intensity of 20 (A, B) and 50 Oe (C, D). Scale bars in A and B are 5 µm and 500 nm, respectively. Scale bars in C and D are 5 µm.

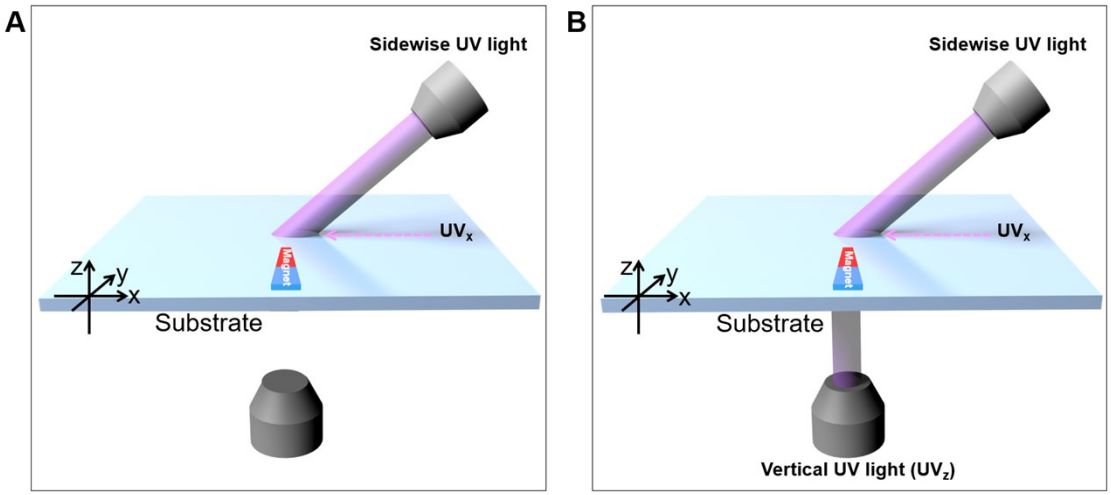

Fig. S4 Schematic illustration of the experimental devices with (A) a single sidewise UV light and (B) with the superimposed sidewise and vertical (UV_z) lights. UV_x represents the horizontal projection of the incident sidewise UV light on the substrate.

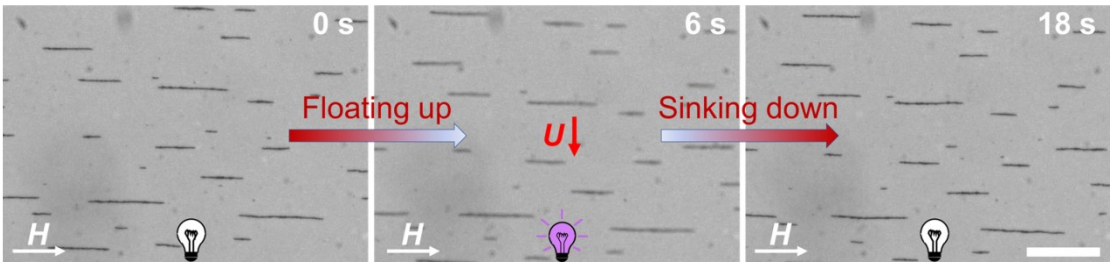

Fig. S5 Time-lapse microscopic images depicting the floating of the MB@TiO_2 MMAs during phototaxing under a single sidewise UV light (without UV_z). The *I* of the sidewise UV light and C_f are 0.16 W cm^{-2} and 2.5 wt.%, respectively. Scale bar, 50 μm.

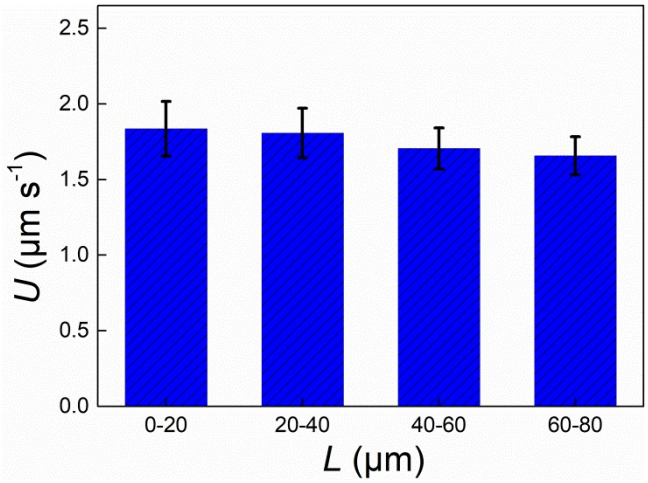

Fig. S6 The *U* of the MB@TiO_2 MMAs with different lengths (*L*). The *I* of the sidewise UV light and C_f in this experiment are 0.41 W cm^{-2} and 2.5 wt.%, respectively.

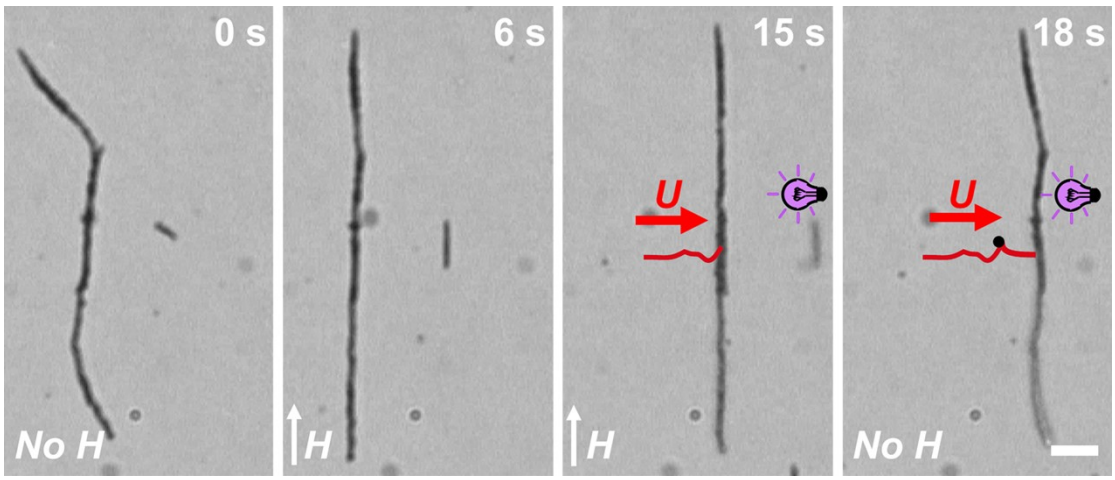

Fig. S7 Time-lapse microscopic images illustrating the deformation and phototactic motion of a typical MB@TiO_2 MMA formed under the external *H* with a high intensity of 50 Oe, revealing that it can not disassemble into dispersed motors after the *H* is removed. The *I* of the sidewise UV light and C_f in this experiment are 0.41 W cm^{-2} and 2.5 wt.%, respectively. Scale bar, 10 μm.

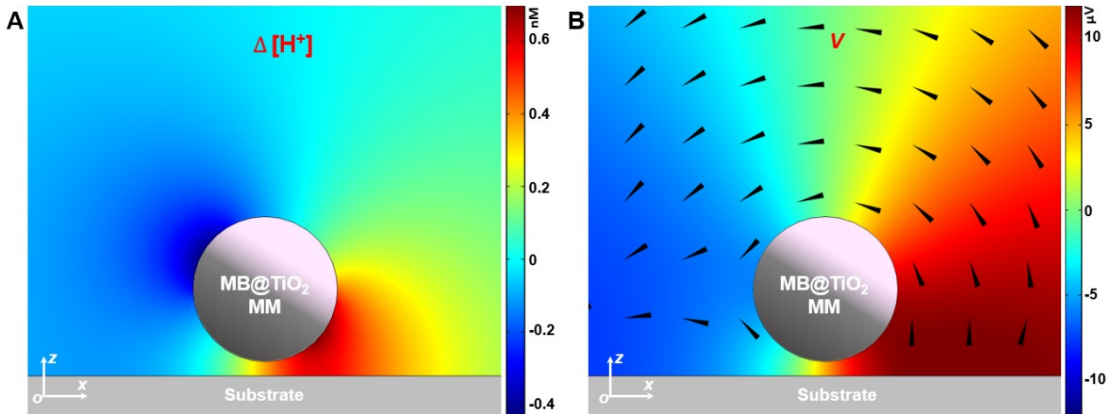

Fig. S8. Numerical simulations of (A) the $[H^+]$ increment ($\Delta[H^+]$) and (B) the electric potential (*V*) around an MB@TiO_2 MMA in the *x*-*z* plane. Black triangles in B represent the direction of the local electric field (*E*).

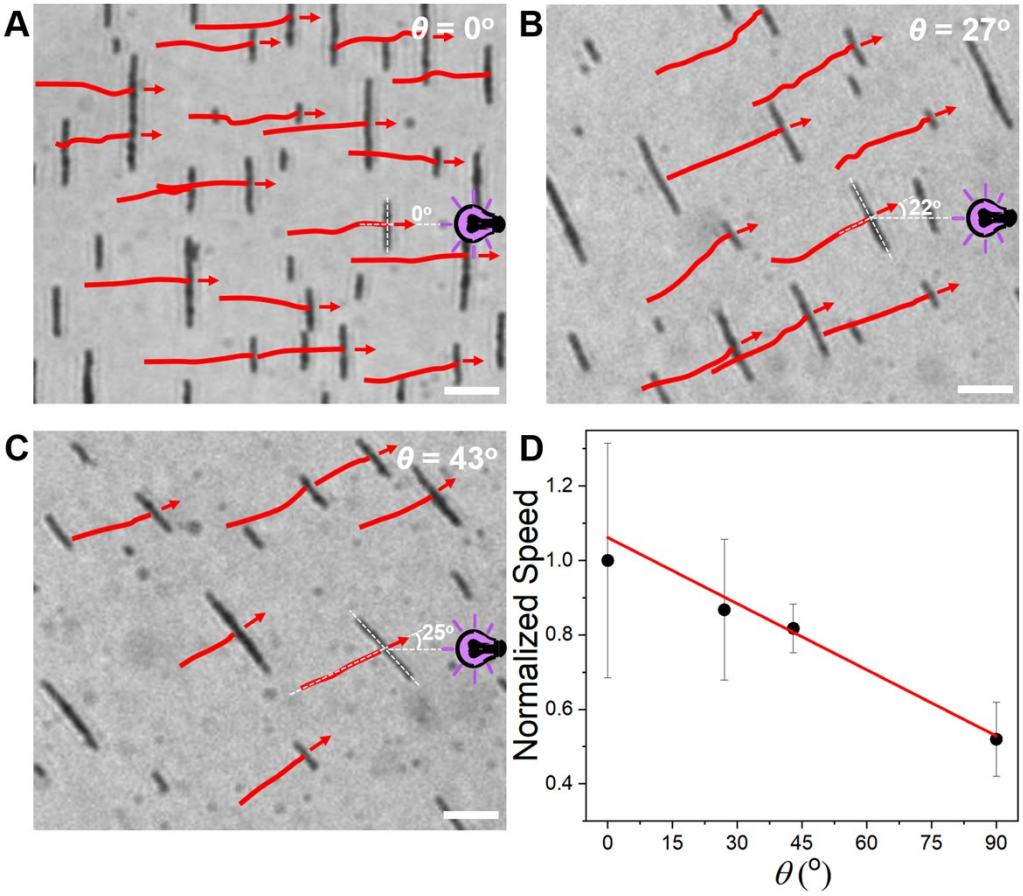

Fig. S9. (A-C) Trajectories of MB@TiO_2 MMAs with different ϑ of 0° (A), 27° (B) and 43° (C), respectively, depicting their increasing migration angle with ϑ. (D) The normalized speed of the MB@TiO_2 MMAs as a function of ϑ. Scale bars in A-C, 10 μm.

Supplementary Videos

Video S1. Dynamic assembly/disassembly behaviors and phototactic flocking of the MB@TiO_2 MMs in response to the external *H* and the sidewise UV irradiation.

Video S2. Floating of the MB@TiO_2 MMAs when phototaxing under an oblique downward UV light.

Video S3. Phototactic flocking of the MB@TiO_2 MMAs at different C_f.

Video S4. Phototactic flocking of the MB@TiO_2 MMAs at different *I*.

Video S5. Phototactic motions of single MB@TiO_2 MMs and MB@TiO_2 MMAs.

Video S6. Phototactic flocking of the MB@TiO_2 MMAs with different φ of the failed individuals.

Video S7. Phototactic flocking of a typical MB@TiO_2 MMA along a predesigned path by adjusting its ϑ.

Video S8. Phototactic flocking of the MB@TiO_2 MMAs when bypassing a rectangular-prism obstacle utilizing their dynamic assembly/disassembly behaviors.

Video S9. Phototactic flocking of the MB@TiO_2 MMAs when passing through the Y-shape branched microchannels utilizing their dynamic assembly/disassembly behaviors.

Video S10. Phototactic flocking of the MB@TiO_2 MMAs when passing through a dumbbell-like microchannel by changing their orientations.

Video S11. Cooperative transport of a large PS microsphere (5 μm) by the MB@TiO_2 MMAs in an open area.

Video S12. Cooperative transport of a large PS microsphere (5 μm) by the MB@TiO_2 MMAs in a confined microchannel.

Video S13. Phototactic flocking of the MB@TiO_2 MMAs when carrying different numbers of the PS microspheres.

Video S14. Sweeping of the PS microspheres (as solid "wastes") out of a specific region by the MB@TiO_2 MMAs.

References

1 B. Jang, W. Wang, S. Wiget, A. J. Petruska, X. Chen, C. Hu, A. Hong, D. Folio, A. Ferreira, S. Pane and B. J. Nelson, *ACS Nano*, 2016, **10**, 9983-9991.

2 W. Duan, R. Liu and A. Sen, *J. Am. Chem. Soc.*, 2013, **135**, 1280-1283.